Research paper

Effects of Denticity and Ligand Rigidity on Reactivity of Copper Complexes with Cumyl Hydroperoxide

Bruce J. Pella, Jens Niklas, Oleg G. Poluektov, Anusree Mukherjee

PII: S0020-1693(18)30916-2
DOI: https://doi.org/10.1016/j.ica.2018.07.035
Reference: ICA 18381

To appear in: *Inorganica Chimica Acta*

Received Date: 14 June 2018
Revised Date: 22 July 2018
Accepted Date: 23 July 2018

Please cite this article as: B.J. Pella, J. Niklas, O.G. Poluektov, A. Mukherjee, Effects of Denticity and Ligand Rigidity on Reactivity of Copper Complexes with Cumyl Hydroperoxide, *Inorganica Chimica Acta* (2018), doi: https://doi.org/10.1016/j.ica.2018.07.035

Effects of Denticity and Ligand Rigidity on Reactivity of Copper Complexes with Cumyl Hydroperoxide

Bruce J. Pella[1], *Jens Niklas*[2], *Oleg G. Poluektov*[2], *Anusree Mukherjee*[1]*,

1. Department of Chemistry, University of Alabama in Huntsville, 301 Sparkman Dr NW, Huntsville, AL 35899
2. Chemical Science and Engineering Division, Argonne National Laboratory, 9700 S. Cass Avenue, Lemont, IL 60439

KEYWORDS: Copper coordination chemistry, oxidation reactions, complex characterization, O-O bond cleavage mechanism, cumyl hydroperoxide

ABSTRACT

Cu(II) complexes bearing N2/Py2 tetradentate ligands consisting of two pyridyl arms and a flexible ethyldiamine backbone, [(BPMEN)Cu(ClO_4)$_2$] (**1**), with rigid cyclohexyl backbone [(BPMCN)Cu(ClO_4)$_2$] (**2**), and substituted with bispyrrolidyl [(PDP)Cu(ClO_4)$_2$] (**3**), and Cu(II) complex bearing N2/Py3 pentadentate ligand, [(TPMEN)Cu(ClO_4)$_2$] (**4**), were synthesized and structurally characterized. Reactivity of **1-4** with cumyl hydroperoxide was investigated to study the effects of ligand rigidity and denticity on the mechanism of O-O bond cleavage. Results presented herein illustrate that **1-3** favors homolysis, however **4** showed little to almost no impact on O-O bond cleavage.

Introduction

Synthetic copper-coupled oxidations have attracted considerable attention in multiple scientific disciplines due in part to their prevalence in biological systems and capability to perform diverse functional group transformations.[1-3] The diversity of biological and synthetic Cu-coupled oxidation processes demonstrates Cu center reactivity can be tuned with coordinated ligands through steric and electronic effects.[4] Among many important roles exhibited by Cu in biology of particular interest are two noncoupled binuclear copper enzymes, dopamine-β-monooxygenase (DβM) and peptidyl-α-hydroxylating monooxygenase (PHM), due to their ability to activate O_2 and accomplish hydroxylation of carbon-hydrogen bonds of their respective substrates.[5,6] Although the mechanism of enzymatic action for PHM and DβM has been thoroughly investigated, the identity and formation of the reactive intermediate responsible for C-H bond hydroxylation is still under debate.[7] Particularly the mechanism of the cleavage of the O-O bond by mono-nuclear Cu-center remains to be established.

In literature synthetic metal complexes and their reactivity toward oxygen has shed important insights about enzyme mechanism. Moreover, metal alkylperoxo complexes have been synthesized to understand mechanism of O-O bond scission (Figure 1). Investigations into Cu(II)-alkylperoxo species may elucidate reaction pathways involved in dioxygen activation by enzymes and synthetic small molecule copper complexes. In 1993, Kitajima *et al.* characterized the first crystal structure for monomeric Cu-alkylperoxo intermediate (LCu(II)-OOR, where R = Cm) by reacting cumyl hydroperoxide (CmOOH) with a bis(μ-hydroxo)copper(II) complex, $[Cu^{II}(HB(3,5\text{-}iPr_2pz)_3)]_2(OH)_2$ in pentane/octane mixture.[8] Since then, considerable research with LCu(II)-OOR complexes has been conducted in order to determine the relationship between structure and reactivity.[9-14] These LCu(II)-OOR complexes have been generated at sub-zero

temperatures and display electrophilic reactivity with external substrates such as 1,4-cyclohexadiene upon thermolytic cleavage of the peroxide (O-O) bond.

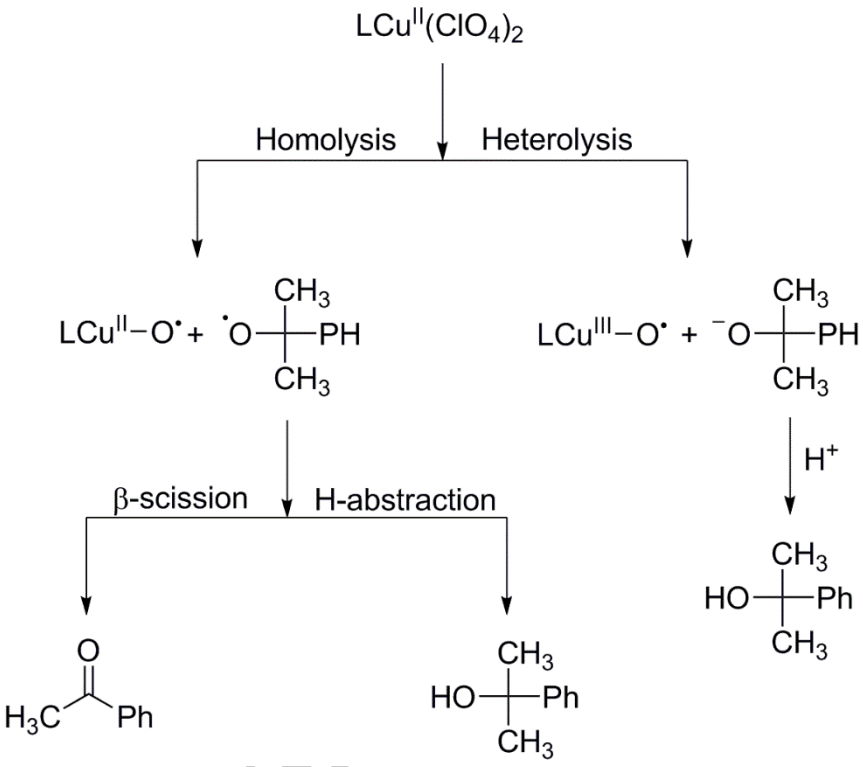

Figure 1: $LCu^{II}(ClO_4)_2$ homolytic and heterolytic O-O bond cleavage mechanisms.

In this study, we investigated the reactivity of cumyl hydroperoxide with three Cu(II) complexes bearing bispicen(N2/Py2) ligands and one Cu(II) complex bearing an N2/Py3 ligand. In order to examine the effect of ligand strain on O-O bond cleavage, the three Cu(II) complexes with N2/Py2 ligands were strategically designed with varied backbone rigidity. The Cu(II) center of $[Cu(BPMEN)(ClO_4)_2]$ (**1,** Figure 2) is ligated to two pendant arms bearing heterocyclic pyridines and to two tertiary amines of a flexible ethyldiamine backbone. In $[Cu(BPMCN)(ClO_4)_2]$ (**2**), the ethyldiamine backbone was substituted with a cyclohexyl variant and $[Cu(PDP)(ClO_4)_2]$ (**3**) was designed with rigid cyclic substituents to replace the flexible

ethyldiamine backbone present in **1**. Additionally, an N5-pentadentate Cu complex bearing an additional pendant arm, [Cu(TPMEN)(ClO_4)$_2$] (**4**), was designed to evaluate the effect of increased denticity on O-O bond cleavage pathway.

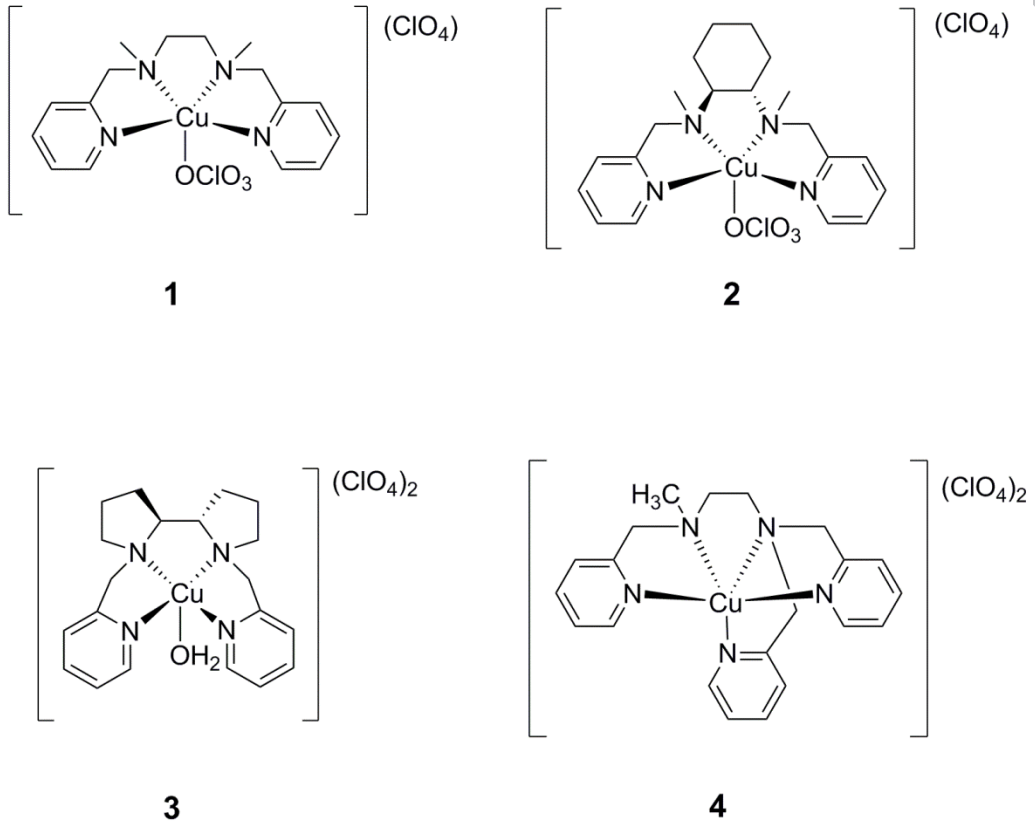

Figure 2. N-polydentate copper complexes, [Cu(BPMEN)(ClO_4)$_2$] (**1)**, [Cu(BPMCN)(ClO_4)$_2$] (**2**), [Cu(PDP)(ClO_4)$_2$] (**3**) and [Cu(TPMEN)(ClO_4)$_2$] (**4)** presented in this work.

Experimental Methods

1.1 Materials

All chemicals and solvents used for syntheses and reactivity studies were acquired from standard commercial suppliers (Fisher Scientific and Millipore Sigma) and used without

further purification. ^{1}H-NMR spectra were recorded with a 500 MHz Varian INOVA spectrometer equipped with a 5 mm Penta (H, C, N, P, D) PFG VT probe using listed deuterated solvents at 25 °C. Mass spectra were recorded with a LTQ Orbitrap XL Hybrid FT Mass Spectrometer in positive ion mode using MeCN or MeOH as solvent. UV-vis absorption spectra were recorded using an Agilent Cary 8454 UV-vis spectrophotometer with dual deuterium and tungsten lamps equipped with Unisoku USP-203 cryostat. Reaction products were characterized and identified using an Agilent 6890 Gas Chromatograph equipped with Agilent 5973 Network Mass Selective Detector and Flame Ionization Detector. Continuous wave (CW) X-band (9 - 10 GHz) EPR experiments were carried out with a Bruker ELEXSYS II E500 EPR spectrometer (Bruker Biospin, Rheinstetten, Germany), equipped with a TE_{102} rectangular EPR resonator (Bruker ER 4102ST). A helium gas-flow cryostat (ICE Oxford, UK) and an intelligent temperature controller (ITC503; Oxford Instruments, UK) were used for measurements at cryogenic temperatures (T = 50 K). Modulation amplitude was 0.6 mT and microwave power was 0.5 mW. Data processing was done using Xepr (Bruker BioSpin, Rheinstetten) and Matlab 7.11.2 (The MathWorks, Inc., Natick) environment. Simulations were performed using the EasySpin software package.[15] Elemental analyses were conducted by Atlantic Microlab, Inc. located in Norcross, GA. X-Ray crystallographic data were collected using a XtaLAB Synergy, Dualflex, HyPix diffractometer equipped with Oxford Cryosystems low-temperature device, operating at T = 100.01(10) K, located at the Emory University – X-Ray crystallographic facility.

Caution! Although no problems occurred in this work, perchlorate salts mixed with organic compounds can be explosive. All necessary safety precautions should be followed.

1.2 Synthesis BPMEN

Synthesis of [N,N'-Dimethyl-N,N'-bis-(pyridine-2-ylmethyl)-1,2-diaminoethane] was taken from a previously reported procedure.[16] 2-(chloromethyl)pyridine hydrochloride (1.501 g, 9.15 mmol) dissolved in 5 mL deionized (DI) water was added dropwise to an aqueous solution containing K_2CO_3 (2.556 g, 18.49 mmol) dissolved in 7.5 mL DI water. The resulting mixture was stirred for 30 minutes. The mixture was extracted with CH_2Cl_2 (3 × 10 mL). The organic phase was collected and dried with anhydrous Na_2SO_4. The dried solution was concentrated *in vacuo* to afford orange oil. A solution containing N,N'-dimethylethylenediamine (0.471 mL, 4.38 mmol) in 15 mL CH_2Cl_2 was added dropwise to the aforementioned orange oil dissolved in 5 mL CH_2Cl_2. An aqueous solution containing NaOH (0.311 g, 7.78 mmol) dissolved in 7.6 mL DI water was slowly added to organic mixture and stirred at room temperature. After 60 hours, a second portion of NaOH solution (0.318 g, 7.95 mmol) was quickly added to the mixture. The combined mixture was extracted with CH_2Cl_2 (3 × 20 mL) and dried with anhydrous Na_2SO_4. The organic solution was concentrated *in vacuo* to afford a brown oil, BPMEN (Yield: 0.631 g, 2.33 mmol, 70%) ^{1}H-NMR (500 MHz, CD_2Cl_2) δ 8.46 (dt, 2H, pyridine ring), 7.80 (m, 2H, pyridine ring), 7.51 (m, 2H, pyridine ring), 7.30 (m, 2H, pyridine ring), 3.70 (m, 4H, -CH_2), 2.66 (m, 4H, -CH_2), 2.27 (s, 6H, -CH_3). ESI-MS (MeOH). Observed *m/z* 271.25 [BPMEN+H^+] (*z* = 1); simulated *m/z* 271.19.

1.3 Synthesis of BPMCN

Synthesis of [N_1,N_2-Dimethyl-N_1,N_2-bis(pyridin-2-ylmethyl)cyclohexane-1,2-diamine] was achieved following a previously reported procedure.[17] 1,2-dimethylcyclohexane-1,2-diamine (164 mg, 1.15 mmol) was dissolved in MeCN (15 mL) in a round-bottom flask.

Triethylamine (780 μL, 5.60 mmol) was added to the solution followed by the addition of 2-(chloromethyl)-pyridine (375 mg, 2.28 mmol). The combined solution was refluxed for 18 hours then cooled to room temperature and concentrated *in vacuo* to yield a crude solid. The crude solid was dissolved in 30 mL CH_2Cl_2 and washed with saturated $NaHCO_3$ (aq, 30 mL). The aqueous wash was extracted with CH_2Cl_2 (2 × 30 mL). The combined organic phase was dried with anhydrous Na_2SO_4. The dried solution was concentrated *in vacuo* to yield a brown oil. The crude product was purified using silica gel chromatography with 86% EtOAc/ 10% MeOH/ 4% NH_4OH to yield a light brown oil, BPMCN. (Yield: 0.143 g, 0.400 mmol, 38%) ^{1}H-NMR (500 MHz, $CDCl_3$) δ 8.48 (t, 2H, pyridine ring), 7.57 (m, 2H, pyridine ring), 7.11 (m, 4H, pyridine ring), 3.81 (m, 4H, -CH_2), 2.65 (m, 2H, -CH), 2.28 (s, 6H, -CH_3), 2.01 (m, 2H, -CH_2), 1.75 (m, 2H, -CH_2). ESI-MS (MeCN). Observed *m/z* 325.24 [BPMCN+H^+] (*z* = 1); simulated *m/z* 325.24.

1.4 Synthesis of PDP

Synthesis of [(-)-2-(((S)-2-((S)-1-(pyridine-2-yl)pyrrolidin-1-yl)methyl)pyridine] was taken from a previously reported procedure.[18] A 50 mL round-bottom flask was charged with (S,S)-2,2'-bispyrrolidine tartrate (1.007 g, 2.92 mmol), 30 mL DI water, and 30 mL CH_2Cl_2. Solid NaOH pellets (0.887 g, 22.18 mmol) were added and dissolved. 2-picolyl chloride•HCl (1.245 g, 7.59 mmol) was dissolved in the solution. After stirring for 18 hours at room temperature, the reaction mixture was diluted with 1 M NaOH. The aqueous layer was extracted with CH_2Cl_2 (3 × 50 mL). The combined organic phase was dried with anhydrous $MgSO_4$ and concentrated *in vacuo* to afford a brown oil. The crude ligand was purified using silica gel chromatography with 93% CH_2Cl_2/ 5% MeOH/ 2% NH_4OH, washed with 1 M NaOH, dried over anhydrous $MgSO_4$, and concentrated *in vacuo* to yield a yellow oil, PDP.

(Yield: 0.454 g, 1.41 mmol, 48%) ^{1}H-NMR (500 MHz, $CDCl_3$) δ 8.50 (m, 2H, pyridine ring), 7.60 (td, 2H, pyridine ring), 7.40 (d, 2H, pyridine ring), 7.11 (dd, 2H, pyridine ring), 4.19 (d, 2H, -CH_2), 3.51 (d, 2H, -CH_2), 3.00 (p, 2H, pyrrolidine –CH_2), 2.80 (p, 2H, pyrrolidine –CH_2), 2.24 (q, 2H, pyrrolidine –CH_2), 1.72 (m, 8H, pyrrolidine –CH_2). ESI-MS (MeCN). Observed *m/z* 323.22 [PDP+H^+] (*z* = 1); simulated *m/z* 323.22.

1.5 Synthesis of TPMEN

Synthesis of [N,N,N'-Tris(2-pyridylmethyl)-N'-methylethylenediamine] was taken from a previously reported procedure.[19] 2-Picolyl chloride hydrochloride (2.99 g, 30.4 mmol) was dissolved in 23 mL 10 N NaOH (9.19 g, 230 mmol) aqueous solution. N-Methylethylenediamine (0.473 mL, 38.2 mmol) was added dropwise to the mixture which was then stirred at room temperature for three days. The upper oil layer was separated and dissolved in 20 mL CH_2Cl_2, washed with DI water (3 × 20 mL). The organic solution was dried with anhydrous $MgSO_4$ and concentrated *in vacuo* to yield a brown oil. The crude ligand was purified using silica gel chromatography with 90% $CHCl_3$/ 10% MeOH and concentrated *in vacuo* to yield a yellow oil, TPMEN. (Yield: 0.174 g, 0.500 mmol, 13%). ^{1}H-NMR (500 MHz, CD_2Cl_2) δ 8.49 (m, 3H, pyridine ring), 7.64 (m, 6H, pyridine ring), 3.83 (m, 4H, -CH_2), 3.64 (s, 2H, -CH_2), 2.72 (m, 4H, -CH_2), 2.21 (s, 3H, -CH_3). ESI-MS (MeOH). Observed *m/z* 348.33 [TPMEN+H^+] (*z* = 1); simulated *m/z* 348.22.

*1.6 Synthesis of [Cu(BPMEN)(ClO_4)$_2$] (**1**)*

The ligand BPMEN (0.271 g, 1.00 mmol) was dissolved in 10 mL MeOH and combined with a 5 mL MeOH solution containing Cu(II) $(ClO_4)_2$ •$6H_2O$ (0.370 g, 1.00 mmol) and stirred for

30 minutes. The combined solution was allowed to slowly evaporate to produce [(BPMEN)Cu(ClO_4)$_2$]. (Yield: 0.307 g, 0.576 mmol, 58%) UV-vis (MeCN) λ_{max} 624 nm (ε = 260 M^{-1} cm^{-1}). ESI-MS (MeCN). Observed *m/z* 333.11 [(BPMEN)Cu] (*z* = 1), 432.06 [(BPMEN)Cu(ClO_4)] (*z* = 1) ; simulated *m/z* 333.11, 432.06.

*1.7 Synthesis of [Cu(BPMCN)(ClO_4)$_2$] (**2**)*

The ligand, (BPMCN) (0.143 g, 0.441 mmol) was dissolved in 3 mL MeOH and combined with a 3 mL MeOH solution containing Cu(II) (ClO_4)$_2$ •6H_2O (0.163 g, 0.440 mmol) and stirred for two hours. A light blue precipitate was filtered and washed with Et_2O and dried *in vacuo* to produce [(BPMCN)Cu(ClO_4)$_2$]. (Yield: 0.125 g, 0.211 mmol, 48%) UV-vis (MeCN) λ_{max} 606 nm (ε = 255 M^{-1} cm^{-1}). ESI-MS (MeCN): Observed *m/z* 486.11 [(BPMCN)Cu(ClO_4)] (*z* = 1); simulated *m/z* 486.11. Elemental Analysis: Observed - C, 40.96; H, 4.74; Cl, 11.93; N, 9.58. Calculated for $C_{20}H_{28}Cl_2CuN_4O_8$ - C, 40.93; H, 4.81; Cl, 12.08; N, 9.55.

*1.8 Synthesis of [Cu(PDP)(ClO_4)$_2$] (**3**)*

The ligand, (PDP) (0.454 g, 1.41 mmol) was dissolved in 5 mL MeOH and combined with a 5 mL MeOH solution containing Cu(II) (ClO_4)$_2$ •6H_2O (0.532 g, 1.41 mmol) and stirred for two hours. A purple precipitate was filtered and washed with Et_2O and dried *in vacuo.* The purple precipitate was dissolved in MeOH and recrystallized by slow diffusion with THF to produce [(PDP)Cu(ClO_4)$_2$]. (Yield: 0.487 g, 0.833 mmol, 59%) UV-vis (MeCN) λ_{max} 587 nm (ε = 211 M^{-1} cm^{-1}). ESI-MS (MeCN): Observed *m/z* 484.09 [(PDP)Cu(ClO_4)$^+$] (*z* = 1);

simulated *m/z* 484.09. Elemental Analysis: Observed – C, 39.96; H, 4.52; Cl, 11.70; N, 9.37. Calculated for [CuPDP]$(ClO_4)_2$•(H_2O) – C, 39.84; H, 4.68; Cl, 11.76; N, 9.29.

*1.9 Synthesis of [Cu(TPMEN)$(ClO_4)_2$ (**4**)*

The ligand, (TPMEN) (0.161 g, 0.463 mmol) was dissolved in 10 mL MeOH and combined with a 10 mL MeOH solution containing Cu(II) $(ClO_4)_2$ •$6H_2O$ (0.177 g, 0.477 mmol) and stirred for 30 minutes. A light blue precipitate was filtered and washed with Et_2O and dried *in vacuo* to produce [(TPMEN)Cu$(ClO_4)_2$]. (Yield: 0.161 g, 0.264 mmol, 57%) UV-vis (MeCN) λ_{max} 687 nm (ε = 268 M^{-1} cm^{-1}). ESI-MS (MeCN): Observed *m/z* 509.09 [(TPMEN)Cu(ClO_4)] (*z* = 1); simulated *m/z* 509.09.

1.10 Cumyl hydroperoxide reactivity at low temperature

Anhydrous MeCN was purged with N_2 gas with stirring for 30 minutes to establish anaerobic conditions. To a solution containing the **1** (1 mM) in anhydrous MeCN in a quartz 1 cm path length UV-vis cell sealed with a rubber septum and purged with N_2 gas placed in cryostat holder at -20 °C for several minutes to reach thermal equilibrium (± 0.5 °C), a solution containing triethylamine (1 mM) in anhydrous MeCN was injected with gastight syringe followed by an injection of a solution containing CmOOH (1 mM) in anhydrous MeCN with gastight syringe. The reaction was monitored for UV-vis spectroscopic changes. The final product solution, where the peak at 385 nm has reached maximum intensity, was taken for an ESI-MS analysis. An aliquot of reaction solution (100 μL) was diluted with anhydrous MeCN (1 mL) and stored at -20 °C. Mass spectra were taken using ESI-MS in positive ion mode, from this cold solution.

In preparation for GC-FID analysis, the reaction solution was warmed to 50 °C until the λ_{max} = ~380 nm peak completely decayed. To this final solution anisole was added as an internal standard (4.5 mM). This solution was passed through a mini-silica column to remove the metal complex and eluted with MeCN (3 mL). The resulting solution was further diluted with MeCN in 1:5 ratio and measured using GC-FID to determine concentration of acetophenone (AP) and cumyl alcohol (CmOH). For **2**-**4** similar procedure was adopted.

1.11 X-ray crystallography

Single blue plate-shaped crystals of **3**, [(PDP)Cu(ClO_4)$_2$] were recrystallized from methanol by slow evaporation. A suitable crystal (0.18×0.11×0.07 mm3) was cut from a larger specimen and mounted on a loop with paratone oil on a XtaLAB Synergy, Dualflex, HyPix diffractometer. The crystal was cooled to T = 100.01(10) K during data collection. The structure was solved with the ShelXT[20] structure solution program using the Intrinsic Phasing solution method and by using Olex2[21] as the graphical interface. The model was refined with version 2014/7 of ShelXL-2014 using Least Squares minimisation.[20,22]

2. Results and Discussion

Synthesis and Characterization

The syntheses of ligands were performed by following published procedures.[16-19] Copper complexes supported by polydentate amine ligands are known in literature and **1**-**4** were obtained using similar techniques.[16,23] The mixing of equimolar amounts of ligand and copper perchlorate salt in methanol at room temperature resulted solid precipitation that was isolated by filtration. All complexes **1**-**4** were analyzed using different spectroscopic and analytical techniques. Crystal structures of complexes **1** and **2** are reported in literature and they were both isolated in square pyramidal (SP) geometry (Table 1). A previously reported crystal structure of **1** displays the flexible N2/Py2 tetradentate ligand coordinates with the Cu(II) metal center in a distorted square pyramidal geometry (τ = 0.36; where τ is distortion index, and typically defined as 0 for square pyramidal geometry and 1 for trigonal bipyramidal geometry[24]).[16] The crystal structure of **2** displays a square pyramidal geometry (τ = 0.02) with four nitrogen atoms occupying equatorial positions and an oxygen atom from H_2O occupying an axial position.[25] Single crystals of complex **3** suitable for X-ray diffraction resulted from a solution of methanol – tetrahydrofuran at room temperature. Single blue plate-shaped crystals of **3** were isolated and X-ray crystallographic analysis revealed **3** adopts a distorted square pyramidal geometry (τ = 0.17) with four nitrogen atoms occupying equatorial positions and an oxygen atom from H_2O occupying an axial position (Figure 3). To our knowledge this is the first example of Cu-complex supported by PDP ligand and perchlorate counter ion. The Cu-N bond lengths of complex **3** are consistent with reported N4-tetradentate Cu(II) complexes with distorted square pyramidal geometry (Table 1 and Table S2).[26-28] Despite exhaustive efforts, crystals suitable for X-ray crystallographic analysis have not been obtained for **4**.

Table 1: Selected structural parameters for complexes, **1-3**.

Complex	**1**	**2**	**3**
Ligand	BPMEN	BPMCN	PDP
Bond Length (Å)			
Cu-N_{amine}	2.026(2)	2.011(4)	2.002(6)
	2.025(2)	2.010(4)	2.030(5)
Cu-$N_{pyridine}$	1.990(2)	1.994(4)	2.023(6)
	1.998(1)	1.987(4)	1.996(6)
Bond Angle(Degrees)			
Cu-O_1[a]	2.245(2)	2.354 (3)	2.284(6)
N_{pyr}-Cu-N_{amine}	167.8	166.9	166.8
	146.4	165.6	156.4
τ	0.36	0.02	0.17
Reference	[16]	[25]	This work

a. Cu-O_1 bond distances for **1-2** derived from ClO_4 and **3** derived from H_2O.

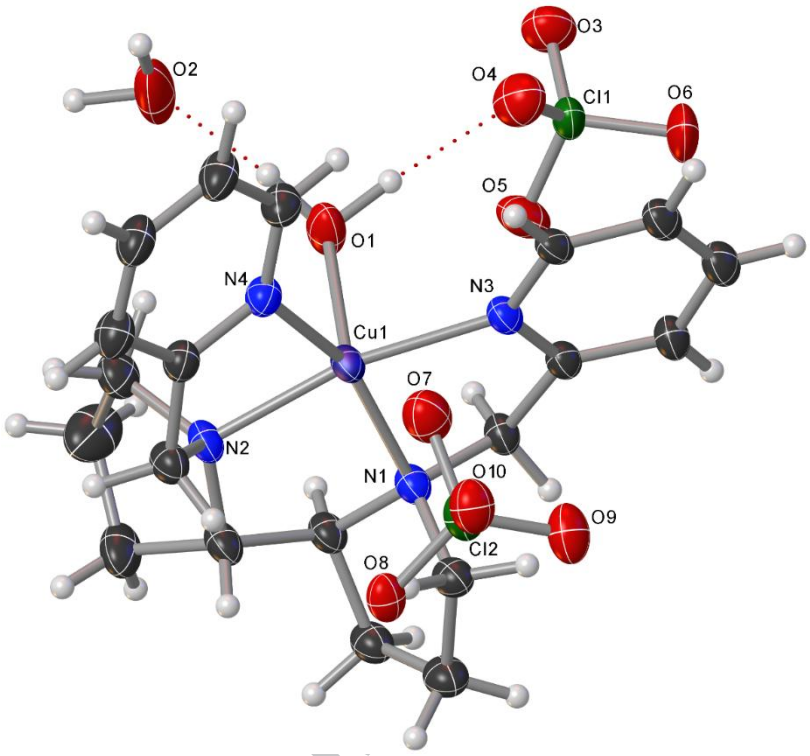

Figure 3: ORTEP view of complex **3** [Cu(PDP)$(ClO_4)_2$]. Hydrogen bonding interactions between axially coordinated water molecule and one of the perchlorate ions are shown by dotted lines.

Optical Spectroscopy

The optical spectra of the complexes **1** and **4** in MeCN are known .[16,23] Complexes **1-3** in MeCN display broad absorption bands in the visible region at 625nm, 606 nm and 587 nm (Figure 4, Table 2), respectively, that correspond to d-d transitions. Complexes **1-3** may coordinate with MeCN in solution to yield a five coordinate complex. The UV-vis spectrum of **4** in MeCN displays a maximum absorption band at 687 nm. While the assignment of coordination geometry

in solution is difficult to determine via optical spectroscopy, the electronic spectra of complexes **1**–**3** are consistent with reported mononuclear Cu(II) complexes in similar ligand environment.[29,30] Electronic spectra of **4** have been published elsewhere and are consistent with previously reported Cu(II) complexes with N5-pentadentate ligand.[23,31-34]

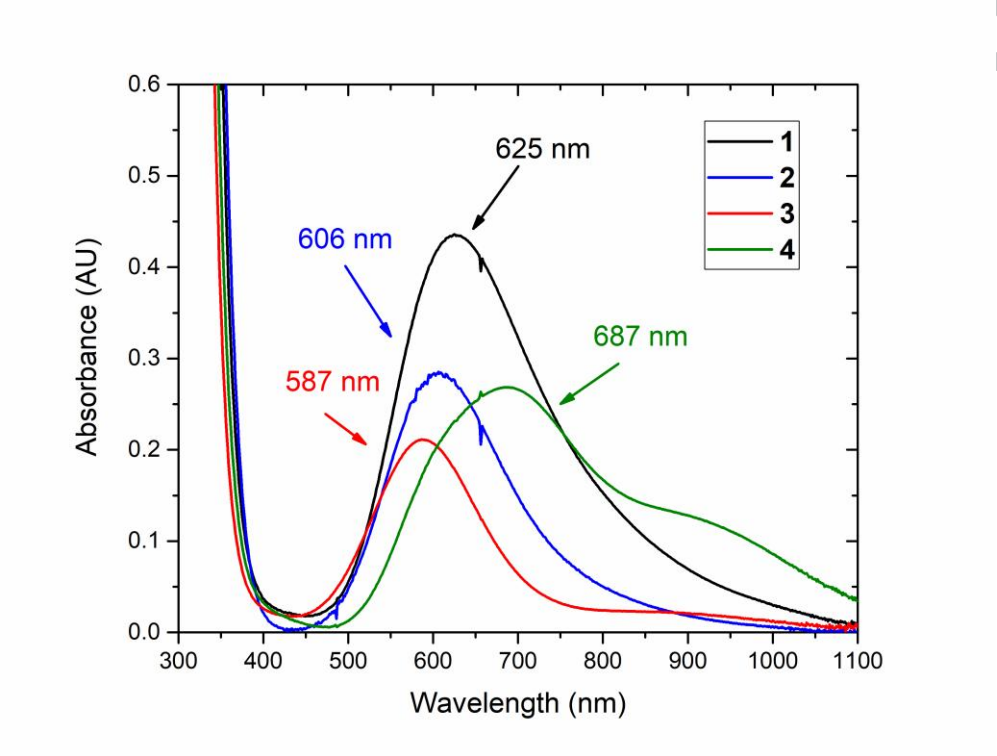

Figure 4: UV-vis absorption spectra of **1-4** (1 mM) in MeCN at room temperature with optical pathlength of 1 cm..

Table 2: Optical and Magnetic parameters for complexes **1 - 4**

Complex	Absorption Maxima nm, (ε M^{-1} cm^{-1}) /MeOH	Absorption Maxima nm, (ε M^{-1} cm^{-1}) /MeCN	g values[a]		Cu hyperfine coupling constants (10^{-4} cm^{-1})	
			$g_{\parallel}$	$g_{\perp}$	$A_{\parallel}$	$A_{\perp}$
1	624 (233)	625 (260)	2.213	2.053	175	31
2	609 (268)	606 (255)	2.216	2.051	180	20
3	593 (191)	587 (211)	2.212	2.047	186	20
4	687 (242), 910 (sh)	687 (268), 907 (sh)	2.209, 2.092, 2.023		158, 50, 35	

a. All EPR measurements were performed in DCM:MeCN solvent mixture (3:1). Cu hyperfine coupling constants are given in 10^{-4} cm^{-1} for the ^{63}Cu isotope. The perpendicular hyperfine coupling constants have a larger error than the parallel hyperfine coupling constants, since the hyperfine structure is not resolved. It was assumed for the simulation that the principal g-tensor axes are collinear with the Cu hyperfine coupling tensor principal axes.

EPR Spectroscopy

EPR spectra of complex **1** was reported from our group.[16] EPR spectra for complex **2-4** were obtained from frozen solution of the complexes in the same solvent system as in our previous study (DCM:MeCN, 3:1, by volume). All three spectra are characteristic of mononuclear Cu(II) complexes in d^9 configuration with S = ½ (Fig. 4). The frozen solution EPR spectra of all Cu(II)-complexes showed a $g_{\parallel}$ value (>2.2) significantly higher than the

other two g-values (<2.1) and resolved Cu hyperfine structure for $A_{\parallel}$ (Cu has two magnetic isotopes, ^{63}Cu and ^{65}Cu, both with nuclear spin I = 3/2, which have very similar magnetic moments and are not resolved in our spectra). Both complexes **2** and **3** showed axial g-tensors and Cu hyperfine tensors. The magnetic resonance parameters are consistent with an electronic ground state, where the unpaired electron resides mainly in the d_{x2-y2} orbital.[35] Complex **3** shows for the perpendicular orientation a partially resolved superhyperfine structure, which we attribute to the four nitrogen atoms of the ligand (I = 1 for ^{14}N). The EPR spectrum of complex **4** exhibits some differences from those of complexes **2** & **3**. The spectrum is not axial anymore, but shows some degree of rhombic distortion. This can be attributed to the presence of five coordinating nitrogen atoms in the ligand vs. four in the other two complexes.

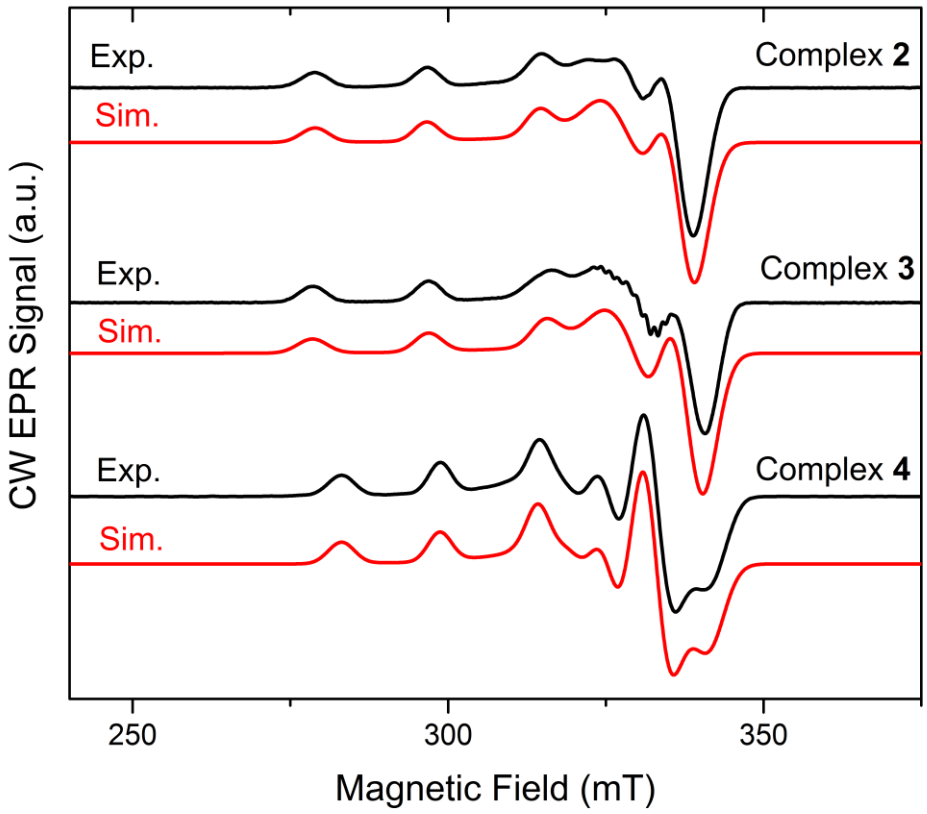

Figure 5: CW X-band EPR spectra obtained from frozen solutions (T = 50 K) of complexes **2**, **3**, and **4** in dichloromethane-acetonitrile solvent mixture (3:1). Spectra shown in black are the experimental spectra. Spectra in red are the corresponding simulations. Simulation parameters are summarized in Table 2.

*Investigation of self-decomposition of cumyl hydroperoxide (CmOOH) with **1-4** at room temperature*

It is well documented in literature that metal-alkylperoxo adduct can shed light about O-O bond cleavage mechanism.[9,11,12] Quantification of CmOOH decomposition products can help determine the nature of O-O bond cleavage. The homolytic and heterolytic cleavage of the O-O bond yield different decomposition products; homolytic O-O bond scission yields radical cumyl-oxyl species that undergoes β-scission to form primarily acetophenone (AP), while heterolytic O-O bond scission yield exclusively cumyl alcohol (CmOH) (Figure 1). To elucidate the effects of coordination and varied ligand rigidity on self-decomposition of LCu(II)-OOCm adduct, reaction of complexes **1-4** in MeCN with excess CmOOH (5 mM) in the presence of base, TEA (2 mM), at room temperature were monitored with UV-visible spectroscopy. Addition of CmOOH to solutions of **1-4** charged with TEA, resulted in slow decay of the peaks associated with the starting material. New absorption features at the 410 nm region developed over the period of 10 hours (Figure 6, S13-15). When the reaction solutions were heated to 50 °C after peak growth at 412 - 415 nm reached maximum intensity, no further spectral changes were observed. Furthermore, it was established that the peak in the 414 nm region does not show significant loss of intensity if the solution was stored at room temperature for a long period of time (24 hrs). Although the peak at 410 nm region is similar to other known LCu(II)-OOCm adduct, no evidence of adduct formation were noted in mass spectrometric analysis of the final solution. The extraordinary stability of the final UV-vis spectra suggests that the species responsible for the maximum absorption bands (λ_{max} = 412 - 415 nm) is a decomposition product produced by the thermal decomposition of the cumylperoxo adduct (LCu(II)-OOCm) derived from complexes **1-4**.

Product analysis of this final solution showed evidence of Cm-OH as a major product in all the cases (Table S1). When the reaction was carried out with 1 equivalent of CmOOH in order to minimize CmOOH sole influence in the decomposition, better results were obtained (Table 3). Comparing the results of decomposition product yields by complexes **1**-**4** with CmOOH decay in absence of any Cu salt, suggests that complexes **1**-**3** all enhance yield of acetophenone (AP) supporting more homolytic cleavage, with the exception of complex **4**. This is probably not very surprising as pentadentate ligand in complex **4** may prevent access of the CmOOH toward the metal center, thus exerting no effect. In order to corroborate our analysis about **4**, CmOOH (1 mM) decomposition was probed in the presence of $Cu(ClO_4)_2$ (1 mM), which primarily produced the heterolytic product, cumyl alcohol (Table S1), comparable to CmOOH decomposition in the presence of **4**.

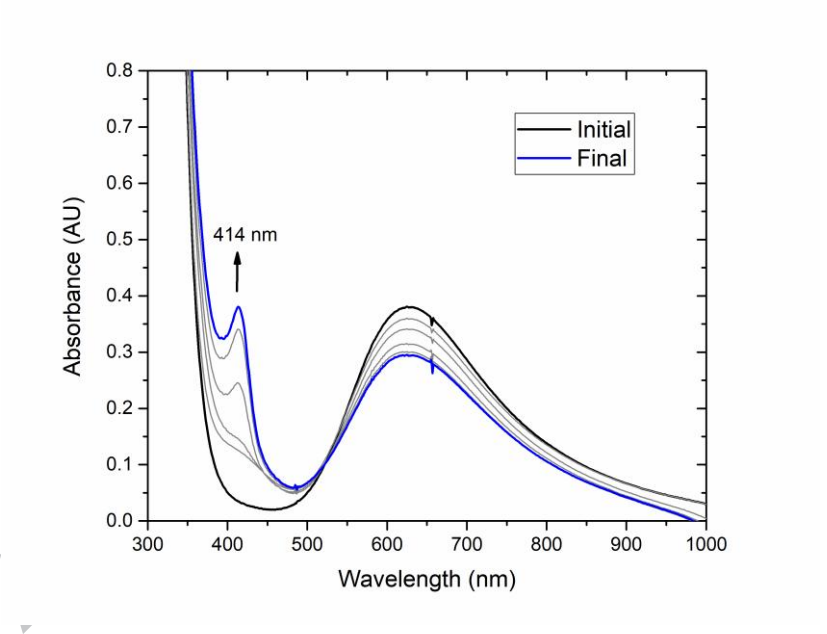

Figure 6: Electronic spectral changes for the reaction of **1** (1 mM) with CmOOH (5 mM) in the presence of TEA (2 mM) in MeCN at 25 °C: initial (black), final (blue) measured in a quartz cuvette (l = 1 cm).

Table 3: Yield of decomposition products from the reactivity of **1-4** with 1 equivalents of CmOOH in the presence of TEA.

	Room Temperature		Low Temperature (-20 °C)		CD_3CN (-20 °C)	
Complex	AP	CmOH	AP	CmOH	AP	CmOH
1	38(3)	62(3)	49(2)	51(6)	68(2)	31(6)
2	30(2)	70(2)	39(3)	61(1)	72(4)	28(2)
3	33(3)	67(4)	28(1)	72(4)	68(8)	32(2)
4	26(2)	74(3)	22(2)	78(2)		
CmOOH	18(2)	82(3)				

*Reactivity of CmOOH with complexes **1-4** at low temperature*

When complexes **1**–**4** were treated with stoichiometric CmOOH in the presence of base, TEA, in MeCN at -20 °C under anaerobic conditions, different spectral signatures were obtained. Upon addition of CmOOH (1 mM), the electronic spectra of **1-4** displayed new maximum absorption bands at 397 nm, 398 nm, 398 nm, and 395 nm, respectively, with a concomitant loss of intensity of d-d transition absorption bands, 625 nm, 606 nm, 587 nm, and 687 nm, respectively (Figure 7a, S17a-19a). The newly formed absorption bands are consistent with maximum absorption bands for previously reported Cu(II)-cumylperoxo complexes and are attributed to a ligand to metal charge transfer (LMCT) transitions. The mass spectrum of the reaction solution of **1** with stoichiometric CmOOH displayed a prominent ion cluster at 484.16 m/*z* assigned to $[(BPMEN)Cu(OOCm)]^+$ (simulated: 484.19 m/z) (Figure S20). However, despite multiple attempts mass spectrometric analysis of the product solution resulting from complexes **2-4** at low temperature showed no evidence of an LCu(II)-OOCm adduct. When solutions of **1-4-**

cumylperoxo complexes were heated to 50 °C, decay of the LMCT absorption bands occurred (Figure 7b, S17b-19b).

Interestingly, when the product solutions of these samples were analyzed after warming to 50 °C, different yield of the decomposition products were obtained (Table 3). Complexes **1** and **2** showed more acetophenone than observed at room temperature; however, complexes **3** and **4** showed no distinct trends in the yield. Furthermore, when these reactions of **1**- **3** were performed using 1 equivalent of CmOOH, in deuterated acetonitrile, yield of the acetophenone enhanced further (Table 3). These observation are in accord with LCu(II)-OOCm self-decomposition mechanism that suggest that acetophenone formation is in competition with H-atom abstraction (Figure 1) and solvent can be a source for H-atom. Thus, deuteration of the solvent, significantly enhances acetophenone yield. Complex **4** was not investigated in CD_3CN as the reactivity trend suggests that **4** has less to no impact with decomposition yield.

a)

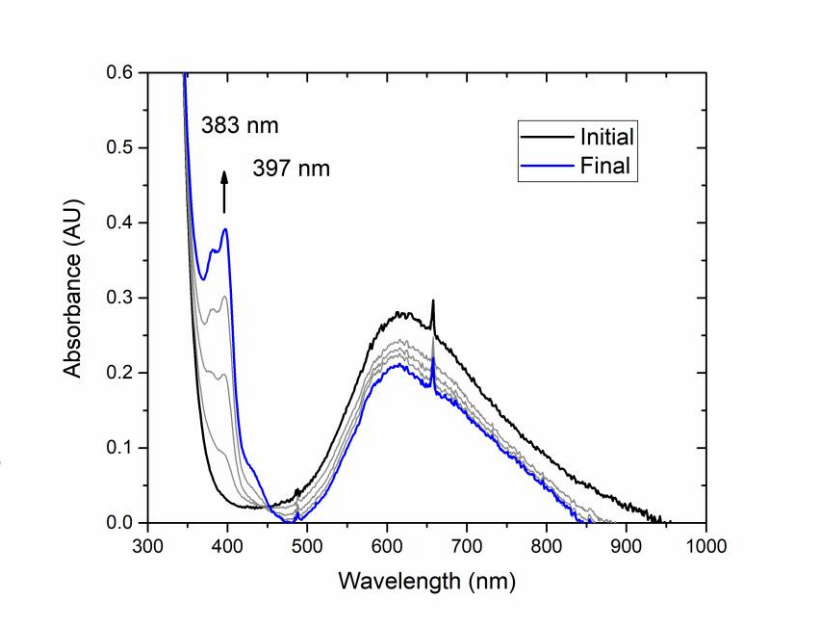

b)

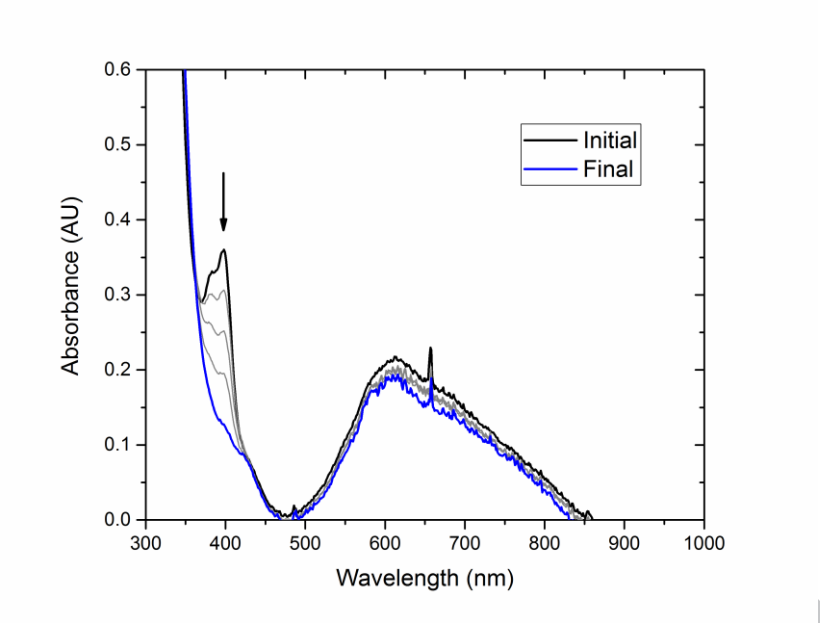

Figure 7: a) Electronic spectra for the reaction of **1** (1 mM) with CmOOH (1 mM) in the presence of TEA (1 mM) in MeCN at -20 °C under anaerobic conditions: initial (black), final (blue). b) Electronic spectra for the thermal decomposition of **1**-cumylperoxo in MeCN at 50 °C under anaerobic conditions over the course of 1 hour: initial (black), final (blue).

Table 4: Reactivity of **1-4** and previously researched Cu(II) complex with CmOOH in the presence of TEA at low temperatures and nature of O-O bond cleavage.

Complex	λ_{max} (nm)	Decomposition Products		Reference
		AP	CmOH	
1	383, 397	49(2)	51(6)	This work
2	398	39(3)	61(1)	This work
3	398	28(1)	72(4)	This work
4	395	22(2)	78(2)	This work
CmOOH (1 equiv.)		18(2)	82(3)	This work
[Cu(bpma)(MeCN)(OOCm)]	465	92		[12]
[Cu(bpa)(MeCN)(OOCm)]	388	76	15	[9]
[Cu(tpa)(OOCm)]	430	83	15	[9]
[Cu(CHDAP)(MeCN)(OOCm)]	475	40	49	[11]

Conclusion

In summary we have synthesized four Cu(II)-complexes supported by polypyridyl ligand with different denticity and backbone rigidity. This paper reports first crystal structure of **3**. Reactivity of these complexes with regard to O-O bond cleavage were pursued using cumyl hydroperoxide as oxidant. The results obtained in this data set suggest complex **4** has no pronounced impact on O-O bond cleavage mechanism of CmOOH, although formation of the near UV band was observed. Among, Cu(II)-complexes with tetradentate ligand (**1**–**3**), various observation were noted. Complexes **1**-**3** all showed preference toward homolysis, the acetophenone yields are significantly improved when solvent is deuterated. However, homolysis yield with these complexes are significantly lower than other known literature evidence (Table 4) but comparable to a recent publication where ligand geometries are restrained.[14] This report illustrates another set of complexes where ligand electronics and steric play important role in O-O bond scission mechanism.

Acknowledgements

B.J.P. and A.M. acknowledge support from University of Alabama in Huntsville. This material is based upon work supported by the National Science Foundation under CHE – 1626172 (X-ray crystallographic analysis). The EPR study was supported by the U.S. Department of Energy, Office of Science, Office of Basic Energy Sciences, Division of Chemical Sciences, Geosciences, and Biosciences, under contract number DE-AC02-06CH11357 at Argonne National Laboratory (J.N. and O.G.P.).

Supporting Information

ESI-MS, NMR spectra, figures for reactivity and crystallographic data and the cif file for **3** are available.

References

(1) Hatcher, L. Q.; Karlin, K. D. Ligand influences in copper-dioxygen complex-formation and substrate oxidations. *Adv. Inorg. Chem.* **2006**, *58*, 131-184.

(2) Mirica, L. M.; Ottenwaelder, X.; Stack, T. D. P. Structure and Spectroscopy of Copper-Dioxygen Complexes. *Chem. Rev. (Washington, DC, U. S.)* **2004**, *104*, 1013-1045.

(3) Lewis, E. A.; Tolman, W. B. Reactivity of Dioxygen-Copper Systems. *Chem. Rev. (Washington, DC, U. S.)* **2004**, *104*, 1047-1076.

(4) Tandon, P. K.; Singh, S. B. Catalytic applications of copper species in organic transformations: a review. *J. Catal. Catal.* **2014**, *1*, 21-34.

(5) Klinman, J. P. Mechanisms Whereby Mononuclear Copper Proteins Functionalize Organic Substrates. *Chem. Rev. (Washington, D. C.)* **1996**, *96*, 2541-2561.

(6) Prigge, S. T.; Kolhekar, A. S.; Eipper, B. A.; Mains, R. E.; Amzel, L. M. Amidation of bioactive peptides: the structure of peptidylglycine α-hydroxylating monooxygenase. *Science (Washington, D. C.)* **1997**, *278*, 1300-1305.

(7) Klinman, J. P. The copper-enzyme family of dopamine β-monooxygenase and peptidylglycine α-hydroxylating monooxygenase: Resolving the chemical pathway for substrate hydroxylation. *J. Biol. Chem.* **2006**, *281*, 3013-3016.

(8) Kitajima, N.; Katayama, T.; Fujisawa, K.; Iwata, Y.; Morooka, Y. Synthesis, molecular structure, and reactivity of (alkylperoxo)copper(II) complex. *J. Am. Chem. Soc.* **1993**, *115*, 7872-7873.

(9) Tano, T.; Ertem, M. Z.; Yamaguchi, S.; Kunishita, A.; Sugimoto, H.; Fujieda, N.; Ogura, T.; Cramer, C. J.; Itoh, S. Reactivity of copper(II)-alkylperoxo complexes. *Dalton Trans.* **2011**, *40*, 10326-10336.

(10) Tano, T.; Sugimoto, H.; Fujieda, N.; Itoh, S. Heterolytic Alkyl Hydroperoxide O-O Bond Cleavage by Copper(I) Complexes. *Eur. J. Inorg. Chem.* **2012**, *2012*, 4099-4103, S4099/4091-S4099/4010.

(11) Kim, B.; Jeong, D.; Cho, J. Nucleophilic reactivity of copper(II)-alkylperoxo complexes. *Chem. Commun. (Cambridge, U. K.)* **2017**, *53*, 9328-9331.

(12) Kunishita, A.; Ishimaru, H.; Nakashima, S.; Ogura, T.; Itoh, S. Reactivity of Mononuclear Alkylperoxo Copper(II) Complex. O-O Bond Cleavage and C-H Bond Activation. *J. Am. Chem. Soc.* **2008**, *130*, 4244-4245.

(13) Chen, P.; Fujisawa, K.; Solomon, E. I. Spectroscopic and Theoretical Studies of Mononuclear Copper(II) Alkyl- and Hydroperoxo Complexes: Electronic Structure Contributions to Reactivity. *J. Am. Chem. Soc.* **2000**, *122*, 10177-10193.

(14) Abe, T.; Morimoto, Y.; Mieda, K.; Sugimoto, H.; Fujieda, N.; Ogura, T.; Itoh, S. Geometric effects on O-O bond scission of copper(II)-alkylperoxide complexes. *J. Inorg. Biochem.* **2017**, *177*, 375-383.

(15) Stoll, S.; Schweiger, A. EasySpin, a comprehensive software package for spectral simulation and analysis in EPR. *J. Magn. Reson.* **2006**, *178*, 42-55.

(16) Singh, N.; Niklas, J.; Poluektov, O.; Van Heuvelen, K. M.; Mukherjee, A. Mononuclear nickel (II) and copper (II) coordination complexes supported by bispicen ligand derivatives: Experimental and computational studies. *Inorg. Chim. Acta* **2017**, *455*, 221-230.

(17) Esarey, S.; Holland, J.; Bartlett, B. 56) EsareDetermining the Fate of a Non-Heme Iron Oxidation Catalyst Under Illumination, Oxygen, and Acid. *Inorg. Chem.* **2016**, *55*, 11040-11049.

(18) Chen, M.; White, M. A Predictably Selective Aliphatic C-H Oxidation Reaction for Complex Molecule Synthesis. *Science* **2007**, *318*, 783-787.

(19) Zhang, L.; Tang, H.; Tang, J.; Shen, Y.; Lingzhi, M.; Radosz, M.; Arulsamy, N. Pentadentate Copper Halide Complexes Have Higher Catalytic Activity in Atom Transfer Radical Polymerization of Methyl Acrylate Than Hexadentate Complexes. *Macromolecules* **2009**, *42*, 4531-4538.

(20) Sheldrick, G. M. SHELXT - Integrated space-group and crystal-structure determination. *Acta Crystallogr., Sect. A: Found. Adv.* **2015**, *71*, 3-8.

(21) Dolomanov, O. V.; Bourhis, L. J.; Gildea, R. J.; Howard, J. A. K.; Puschmann, H. OLEX2: a complete structure solution, refinement and analysis program. *J. Appl. Crystallogr.* **2009**, *42*, 339-341.

(22) Sheldrick, G. M. Crystal structure refinement with SHELXL. *Acta Crystallogr C Struct Chem* **2015**, *71*, 3-8.

(23) Snider, V. G.; Pella, B. J.; Mukherjee, A. Synthesis, characterization, and reactivity of copper complexes supported by the TPMEN ligand framework. *Inorg. Chim. Acta* **2018**, *469*, 447-452.

(24) Addison, A. W.; Rao, T. N.; Reedijk, J.; Van Rijn, J.; Verschoor, G. C. Synthesis, structure, and spectroscopic properties of copper(II) compounds containing nitrogen-sulfur donor ligands: the crystal and molecular structure of aqua[1,7-bis(N-methylbenzimidazol-2'-yl)-2,6-dithiaheptane]copper(II) perchlorate. *J. Chem. Soc., Dalton Trans.* **1984**, 1349-1356.

(25) Zhang, Y.; Xiang, L.; Wang, Q.; Duan, X.-F.; Zi, G. Synthesis, structure, and catalytic activity of chiral Cu(II) and Ag(I) complexes with (S,S)-1,2-diaminocyclohexane-based N4-donor ligands. *Inorg. Chim. Acta* **2008**, *361*, 1246-1254.

(26) Chapman, R. L.; Stephens, F. S.; Vagg, R. S. Studies on the metal-amide bond. II. The crystal structure of the deprotonated copper(II) complex of N,N'-bis(2'-pyridinecarboxamide)-1,2-benzene. *Inorg. Chim. Acta* **1980**, *43*, 29-33.

(27) Samanta, B.; Chakraborty, J.; Choudhury, C. R.; Dey, S. K.; Dey, D. K.; Batten, S. R.; Jensen, P.; Yap, G. P. A.; Mitra, S. New Cu(II) complexes with polydentate chelating Schiff base ligands: Synthesis, structures, characterizations and biochemical activity studies. *Struct. Chem.* **2007**, *18*, 33-41.

(28) Brewer, G.; Brewer, C. T.; Kamaras, P.; Prytkov, S.; Shang, M.; Scheidt, W. R. Synthesis and structural characterization of copper complexes of N4 tetradentate Schiff bases derived from N-alkylated 2-aminobenzaldehyde. Effects of cyclization, oxidation, and dinucleation. *Inorg. Chim. Acta* **2001**, *321*, 175-180.

(29) Brudenell, S. J.; Spiccia, L.; Tiekink, E. R. T. Binuclear Copper(II) Complexes of Bis(pentadentate) Ligands Derived from Alkyl-Bridged Bis(1,4,7-triazacyclononane) Macrocycles. *Inorg. Chem.* **1996**, *35*, 1974-1979.

(30) Massoud, S. S.; Louka, F. R.; David, R. N.; Dartez, M. J.; Nguyn, Q. L.; Labry, N. J.; Fischer, R. C.; Mautner, F. A. Five-coordinate metal(II) complexes based pyrazolyl ligands. *Polyhedron* **2015**, *90*, 258-265.

(31) Lo, W. K. C.; McAdam, C. J.; Blackman, A. G.; Crowley, J. D.; McMorran, D. A. The pentadentate ligands 2PyN2Q and N4Py, and their Cu(II) and Zn(II) complexes: A synthetic, spectroscopic and crystallographic structural study. *Inorg. Chim. Acta* **2015**, *426*, 183-194.

(32) Mukhopadhyay, U.; Bernal, I.; Massoud, S. S.; Mautner, F. A. Syntheses, structures and some electrochemistry of Cu(II) complexes with tris[(2-pyridyl)methyl]amine: [Cu{N(CH2-py)3}(N3)]ClO4 (I), [Cu{N(CH2-py)3}(O-NO)]ClO4 (II) and [Cu{N(CH2-py)3}(NCS)]ClO4 (III). *Inorg. Chim. Acta* **2004**, *357*, 3673-3682.

(33) McLachlan, G. A.; Fallon, G. D.; Martin, R. L.; Spiccia, L. Synthesis, Structure and Properties of Five-Coordinate Copper(II) Complexes of Pentadentate Ligands with Pyridyl Pendant Arms. *Inorg. Chem.* **1995**, *34*, 254-261.

(34) Hathaway, B. J. Correlation of the electronic properties and stereochemistry of mononuclear [CuN4-6] chromophores. *J. Chem. Soc., Dalton Trans.* **1972**, 1196-1199.

(35) Husarikova, L.; Repicka, Z.; Moncol, J.; Valigura, D.; Valko, M.; Mazur, M. Unusual EPR Spectra with Inverse Axial g values of Chlorosalicylate-Cu(II)-2,6-Pyridinedimethanol Complex in Frozen Water-Methanol Solution. *Appl. Magn. Reson.* **2013**, *44*, 571-582.

- Syntheses of N-polydentate copper(II) complexes with varied rigidity and denticity
- Reaction with cumyl hydroperoxide generated absorption bands from 380-420 nm
- Heterolytic cleavage predominates in the presence of tetradentate copper complexes
- Ligand rigidity has a minor effect on cleavage pathway